ELSEVIER

Thinning transitions and fluctuations of freely suspended smectic-A films as studied by specular and diffuse X-ray scattering

E.A.L. Mol[a], G.C.L. Wong[a], J.M. Petit[b], F. Rieutord[b], W.H. de Jeu[a],*

[a] *FOM Institute for Atomic and Molecular Physics, Kruislaan 407, 1098 SJ Amsterdam, The Netherlands*
[b] *UMR 585 CEA-CNRS-Univ. J. Fourier, Departmento de Recherche Fondamentale de la Matière Condensée, CEA-Grenoble, 38054 Grenoble, France*

Abstract

The fluctuations in freely suspended smectic-A films have been studied using specular and diffuse X-ray scattering. Such films thin layer-by-layer above the bulk transition temperature of the smectic-A–nematic phase transition. The electron density profiles obtained from specular reflectivity demonstrate that thinning originates from nematic layers being expelled from the interior of the film. In addition, using diffuse scattering the spectral dependence of the displacement–displacement correlation function could be measured down to molecular dimensions, with a $(2 + 2)$ scattering geometry at a synchrotron source. At long in-plane length scales the fluctuations of the smectic layers were found to be conformal; i.e. top and bottom of the film fluctuated in unison. However, at increasing wave vector transfers, conformality was progressively lost. © 1998 Elsevier Science B.V. All rights reserved.

Keywords: Diffuse X-ray scattering; Liquid crystalline films; Thermal fluctuations

1. Introduction

Smectic-A (SmA) liquid crystals are uniaxial systems possessing long-range orientational order. In addition, the molecules are on average arranged in equidistant layers, while the translational order is liquid like in the other two directions. Since such a system is at its lower marginal dimensionality, the positional order is not truly long range but decays algebraically with position as $r^{-\eta}$. The fluctuations of the smectic layers are responsible for the absence of true long-range order: if $u(r)$ is the layer displacement from its equilibrium position, $\langle u^2(r) \rangle$ is found to diverge logarithmically with the sample size (Landau–Peierls instability) [1]. In practice, it is difficult to observe the loss of long-range order because of the slow logarithmic growth of the fluctuations with the size of the sample [2].

The layered structure of smectic liquid crystals allows the existence of films, which are freely suspended over an aperture in a frame. These films have a well-controlled size and high degree of uniformity, with thicknesses varying from two to over hundreds of layers. This makes them ideal model

* Corresponding author: Tel.: + 31 20 608 1315; fax: + 31 20 668 4106; e-mail: dejeu@amolf.nl.

systems for the investigation of the crossover from three-dimensional to two-dimensional behaviour, as well as the influence of the surfaces on the physical properties [1]. Due to the surfaces such films can be stable above the bulk transition temperature of the SmA to the nematic (N) [3] or isotropic (I) [4] phase transition. Instead of rupturing at the bulk phase transition the films lose layers in discrete steps as a function of temperature. We have investigated freely suspended films close to a second-order bulk SmA–N phase transition using specular reflectivity, which probes the laterally averaged density profile through the film. This allowed us to ascertain the profile of the total fluctuation amplitude, σ_{tot}, in the film just before thinning. This amplitude depends on the collective displacements of the layers as well as the motion of individual molecules within the layers. A strong enhancement of the fluctuations in the centre of the film as compared to those at the surfaces was observed with fluctuation amplitudes of up to 10 Å in the interior. These results support models that assume that upon thinning a molten layer is expelled from the interior of the smectic film.

Recently, the thermal fluctuations of freely suspended films have been studied using diffuse scattering [5], which allows the determination of the interlayer displacement–displacement correlation function $C(R, z, z') = \langle u(\mathbf{R}, z) u(0, z') \rangle$, where $\mathbf{R}$ is in the plane of the film and z along the film normal. This function describes the behaviour of the thermal fluctuations, which depends on the surface tension (γ) and the elastic constants for compression (K) and bending (B) of the smectic layers [6]. At long in-plane length scales these fluctuations were found to be highly correlated, as a result of the slow algebraic decay of the interlayer density–density correlation function. Thus, all the layers fluctuate conformally, i.e. they undulate in unison and $C(R, z, z')$ decays logarithmically with decreasing R. In this case the diffuse scattering is the coherent superposition of scattering from each layer. On the other hand, for $R < R_c \approx 2\sqrt{L\lambda}$ [5], where $\lambda = \sqrt{K/B}$ and L is the thickness of the film, conformality is expected to vanish, starting between top and bottom of the film. The use of a $(2 + 2)$ grazing incidence scattering set-up [7]

allowed measurements of the displacement–displacement correlation function from mesoscopic down to molecular in-plane distances R. The use of this set-up, in combination with a parameter choice that leads to relatively large values of R_c, allowed the first observation of the crossover from conformal to independent thermal fluctuations of the smectic layers.

In the next section, the liquid-crystal is investigated and the experimental conditions are introduced. Section 3 describes the layer-by-layer thinning results, while in Section 4 the results of the diffuse measurements on the crossover to non-conformality are presented.

2. Experimental

The compound investigated is 4,4′-diheptylazoxybenzene (7AB), with structural formula C_7H_{15}–Φ–N_2O–Φ–C_7H_{15}. The bulk phase sequence is Cryst32.4 SmA52.9 N69.9 I (temperatures in degrees centigrade). The SmA–N phase transition [8] is second order. At such a transition the compressional elastic constant B is expected to vanish, or reach a finite small value [1]. 7AB was obtained from Frinton (Vineland, USA) and was recrystallized several times. The freely suspended films covered an area of 28×10 mm^2 determined by four knife-like blades of a rectangular hole in a steel holder. The sample holder was mounted in a cylindrical two-stage oven, which was evacuated and sealed. The thinning experiment has been performed on two films, with original thicknesses of 28 and 46 layers. The films were heated in steps of 0.10°C and allowed to equilibrate at each thickness for at least an hour. No thinning was observed over periods of days when the temperature was constant. Nor did the films thicken when the temperature was lowered. The diffuse X-ray scattering measurements were performed at 52.2 $\pm$ 0.1°C, far enough from the bulk SmA–N phase transition to avoid loss of layers during the experiment.

The layer-by-layer thinning was studied using specular reflectivity on an in-house X-ray set-up, as described in Ref. [5], using X-rays with wave number $|\mathbf{k}| = 4.07$ Å^{-1}. The conformality experiment was performed at the beam-line BM32 at the

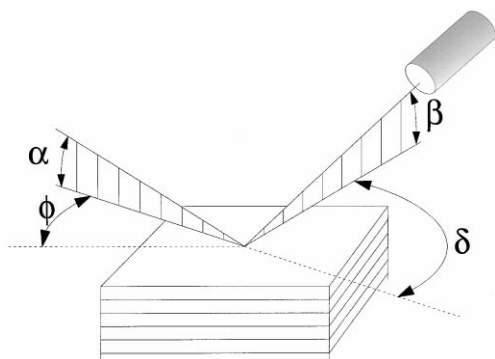Fig. 1. The scattering geometry in a '2 + 2' surface diffraction set-up with specular scans along q_z, varying α and β with respect to the sample surface while keeping them equal ($\delta = \phi = 0$), transverse scans varying q_y at fixed q_z ($\alpha = \beta$), in which the detector is moved out of the scattering plane over an angle δ, while rotating the sample over $\phi = \delta/2$ and finally scans parallel to q_z at an offset q_y.

European Synchrotron Radiation Facility ESRF (Grenoble, France), with $|\boldsymbol{k}| = 9.12\,\text{Å}^{-1}$. Using a so-called (2 + 2) surface X-ray diffractometer [7], as shown in Fig. 1a, the diffuse intensity has been measured by moving the detector and sample out of the plane of specular reflection, while the angles of the incoming and outgoing wave vector were kept constant with respect to the sample surface. Similar geometries have recently been used to perform diffuse scattering measurements of multilayers [9] and amphiphilic films [10]. Three scan types were used: specular scans, diffuse scans parallel to the specular rod and transverse scans perpendicular to the specular rod; in all cases $q_x = 0$. In reciprocal space specular scans probe the scattered intensity along q_z with $q_y = 0$. Transverse scans probe the scattered intensity along q_y at fixed q_z. Finally, in the third type of scans scans q_z is varied at a constant offset q_y. All scans are background subtracted, where the background was measured in scans with no film present. This gave a dynamic range larger than 2×10^{10}. The data were corrected if the footprint of the beam was larger than the sample, for the changing illuminated sample area visible by the detector, and for the polarization factor [7].

The out-of-plane grazing incidence (2 + 2)-scattering set-up does not restrict the accessible in-plane q-range, which is in contrast with the conventional two circle diffractometer set-up for diffuse scattering, where q_x is varied by rocking the sample in the beam. Then a limited in-plane q-range is accessible before the sample blocks either the incident or exit beam. The adapted scattering geometry at a synchrotron source allowed the measurement of the diffuse intensity up to $q_y \approx 1.6\,\text{Å}^{-1}$, corresponding to lateral molecular dimensions ($\approx 4 - 5\,\text{Å}$). Furthermore, transverse scans with large in-plane momentum transfer q_y could be measured at small q_z where the scattered intensity was high. Thus, both correlations between neighbouring and next nearest layers at $q_z = q_0$ and $q_z = q_0/2$, respectively, could be probed, where q_0 indicates the Bragg-position. This in contrast with the set-up used in Ref. [5], where the maximum in-plane momentum transfer, corresponding to $q_x \approx 0.022\,\text{Å}^{-1}$, could effectively be reached at the second Bragg peak where the intensity is low. Note that correlations in q_x and q_y are equivalent, as the SmA samples are uniaxial along the z-axis.

3. Thinning transitions

Fig. 2 shows the temperature of melting $T_{NA}(N)$ of a N layer film. As a function of temperature, melting occurred as a series of discrete transitions. Both the 46 and 28 layer film thinned layer by layer, although only one thinning transition has been measured for the 46 layer film. The 46 layer film lost a layer at $0.9°C$ above the bulk-phase transition, while the thinnest measured film of 12 layers was stable up to $10°C$ above this transition. Note that films with an even number of layers thin layer by layer as well, although in this case two neighbouring inner layers are equivalent.

Reflectivity curves for a 24 layer film at, respectively, $11.6°$, $4.4°$ and $0.1°C$ below $T_{NA}(24) = 56.3°C$ are displayed in Fig. 3. Besides this data the specular reflectivity of a 12 layer film at $63.2°C$, $0.1°C$ below $T_{NA}(12)$, is shown in this figure. The solid line fits are calculated with the reflectivity program SPEEDO [11]. The positions of the Bragg peaks and the Kiessig fringes in the specular reflectivity curve fix d and N, respectively, where $d = 28.75 \pm 0.05\,\text{Å}$. The insets of Fig. 3 show the
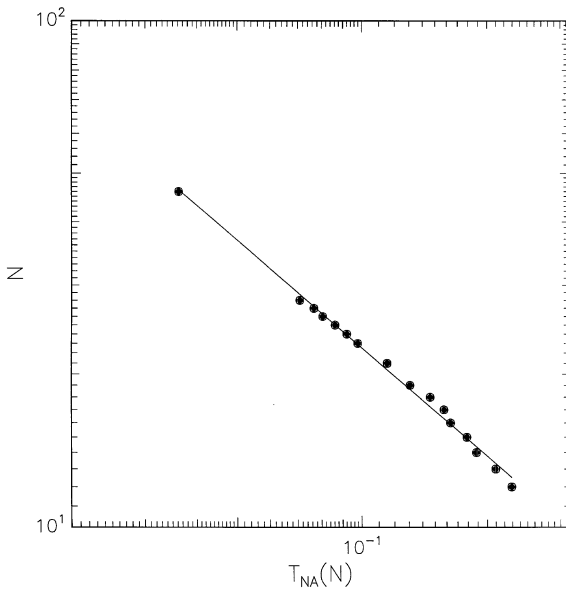
Fig. 2. The number of layers of a freely suspended film versus $T_{NA}(N)$, the highest temperature where the N layer film is stable.

profile of the total amplitude of the fluctuations, or layer roughness, in the film as obtained from the fits [12]. The fluctuations are strongly enhanced in the interior of the film as compared to the surfaces.

The layer thinning data can be described by a simple power law of the form $N(t) = l_0 t^{-\nu}$, where $t = [T_{NA}(N) - T_0]/T_0$ [3,4]. Fig. 2 shows a fit of this power law to the experimental data, which yields the following parameters: $l_0 = 4.9 \pm 0.3$, $\nu = 0.68 \pm 0.03$, and $T_0 = 52.10 \pm 0.05°C$. The value for the exponent can be related to $\xi_\parallel$, the correlation length of the smectic order parameter in the direction parallel to the director [3]. The temperature dependence of $\xi_\parallel$ is also described by a power law with an exponent $\nu_\parallel$. The value obtained for 7AB is in excellent agreement with the critical exponent determined earlier using a Fréedericksz transition technique [13]. It also agrees well with the exponents determined by layer-by-layer thinning experiments [3,4] on other compounds. However, in the case of a second-order SmA–N phase transition T_0 should be equal to T_{NA} whereas our T_0 is 0.8°C lower. This discrepancy is the consequence of the absence of accurate

thick-film data. Inclusion of an only roughly determined single thinning temperature for a 100 layer film gives $T_0 = T_{NA} \pm 0.07°C$, but introduces a larger uncertainty in ν.

Qualitatively, Fig. 3 shows that melting starts in the interior of the film, for the Bragg peaks disappear upon approaching T_{NA}, while the amplitude of the Kiessig fringes is constant. This has been a natural assumption in most theories of layer-by-layer thinning [14], which, however, has not been substantiated experimentally before. The enhanced order at the surfaces of the film is quite distinct in the electron density profiles shown in Fig. 4. In our analysis the melting can be described as a divergence of the amplitude of the total fluctuations, as shown in the insets of Fig. 3. While the amplitude of the fluctuations in the surface layers of the film remains relatively constant at a value of approximately 3.5 Å, it increases in the centre from 5.4 to 9.3 Å upon approaching $T_{NA}(24)$. In the latter case the film is still 0.1°C below the thinning temperature. The data of the 12 layer film in Fig. 3 gives fluctuation amplitudes up to 11.2 Å in the interior layers. These profiles depend on both the contribution of the thermal layer fluctuations and the uncorrelated local molecular disorder: $\sigma_{tot}^2 = \sigma^2 + \sigma_{loc}^2$, where $\sigma = \langle u^2(0,z) \rangle^{1/2}$. Specular reflectivity cannot separate the two contributions, however. As expected the data could be fit using the same molecular form factor at all temperatures for both film thicknesses. This strongly suggests that the disappearance of the second-order Bragg peak is primarily due to the profile of the fluctuations. In conclusion, the layer-by-layer thinning experiment clearly demonstrates a divergence of the amplitude of the fluctuations in the interior of the film upon melting.

4. Crossover to loss of conformality

In order to study the correlation in the thermal fluctuations we continue with the diffuse X-ray scattering experiment. The specular and diffuse longitudinal scans for the 24 layer film are presented in Fig. 5a. At small q_y the film is conformal and the diffuse scattering is the coherent superposition of scattering from each layer, showing maxima and
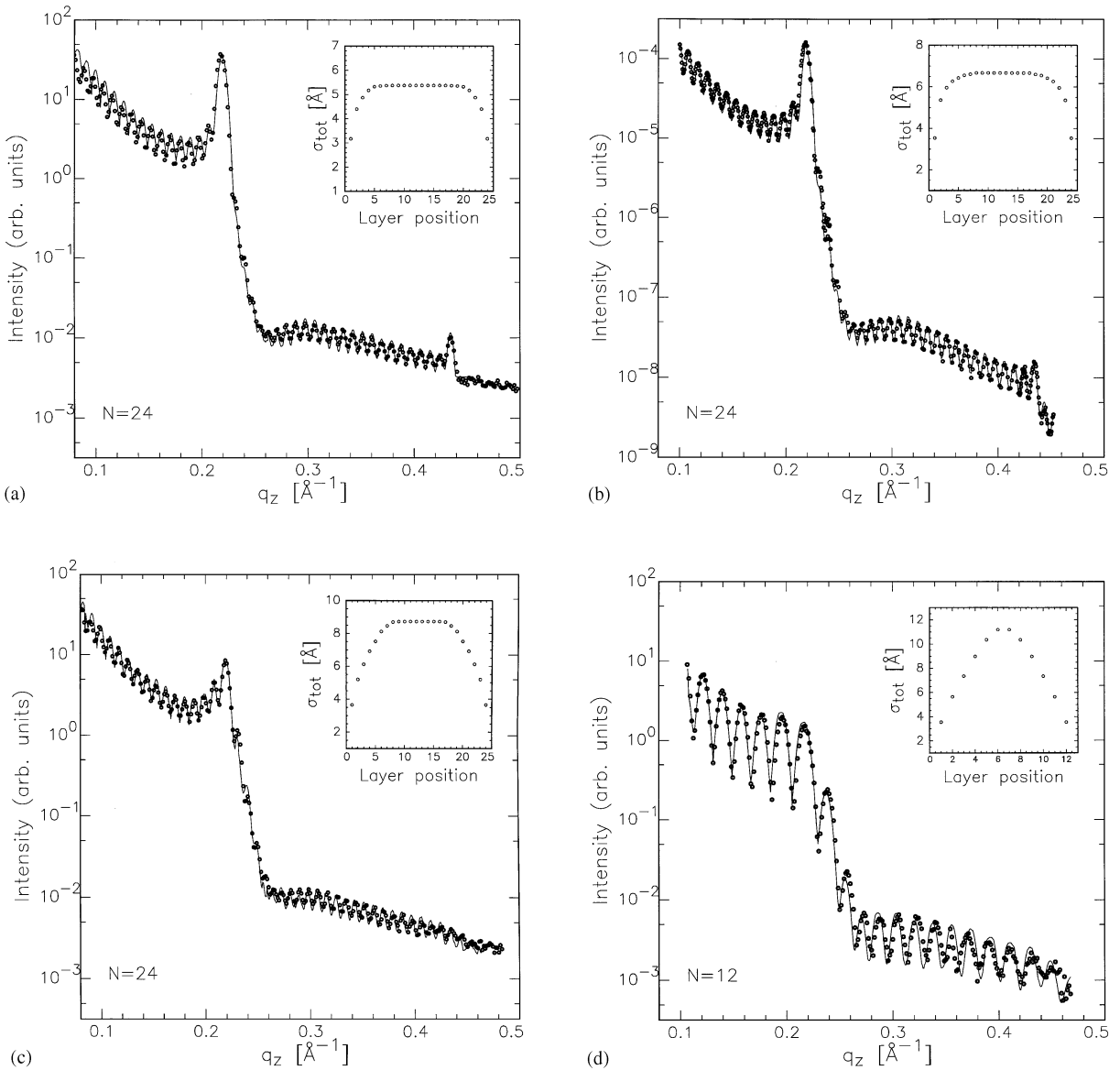
Fig. 3. Specular reflectivity curves with a solid line fit to the data for a 24 layer film at 45.0°C, 52.2°C and 56.2°C, where $T_{NA}(24) = 56.3°C$, and a 12 layer film at 63.0°C, 0.1°C below $T_{NA}(12)$. The inset shows the total amplitude of the fluctuations in the film.

minima at the same positions as the specular reflectivity [15]. The disappearance of the interference fringes with increasing q_y indicates that the top and bottom of the film no longer fluctuate in unison. This disappearance is more apparent in the enlargement of a smaller q_z-range in Fig. 5b. The

persistence of the Bragg peak up to $q_y = 0.0414 \, \text{Å}^{-1}$ ($R \approx 150 \, \text{Å}$), however, shows that lateral correlation between adjacent layers still exists. The broadening and weakening of the Bragg peak reveals that with increasing in-plane momentum transfer more layers fluctuate independently and
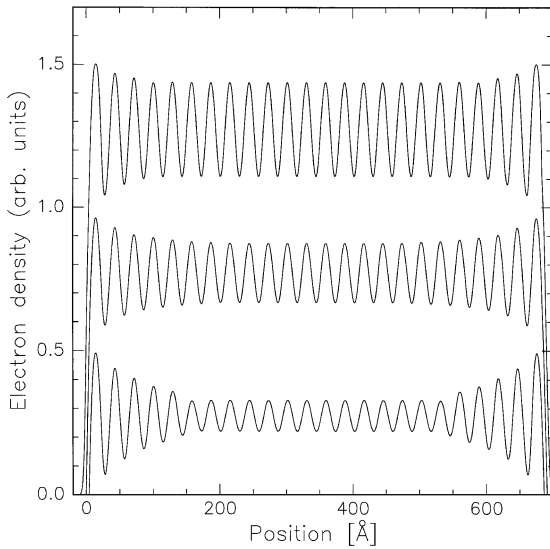
Fig. 4. The electron density profile in a 24 layer film at 45.0°C, 52.2°C and 56.2°C, respectively. The bottom two curves are shifted.

thus less layers are contributing coherently to the diffuse signal.

Additional information about the displacement–displacement correlation function can be obtained from the transverse diffuse scans. Scans were done across the first Bragg peak (q_0), across a sub-harmonic of the Bragg peak ($0.5q_0$) and at an intermediate interference fringe ($0.7q_0$). Transverse scans for a 100 and a 24 layer film of 7AB are shown in Fig. 6. At small q_y the slopes of the transverse scans are approximately parallel at all q_z, therefore all the layers are fluctuating in unison. The development of different slopes in the various scans is the signature of loss of conformality of the thermal fluctuations with increasing in-plane momentum transfer. The slopes are still very similar, even for $R < R_c$, at the Bragg peak and at the sub-harmonic, in particular, for the 100 layer film. Here the dominant contributions to the diffuse scattering are from lateral correlations between adjacent and next nearest layers, respectively. This indicates that lateral correlations between adjacent and next nearest layers persist down to molecular length scales. At the same time the very different slope of the scan at $q_z = 0.7q_0$, where only correlations
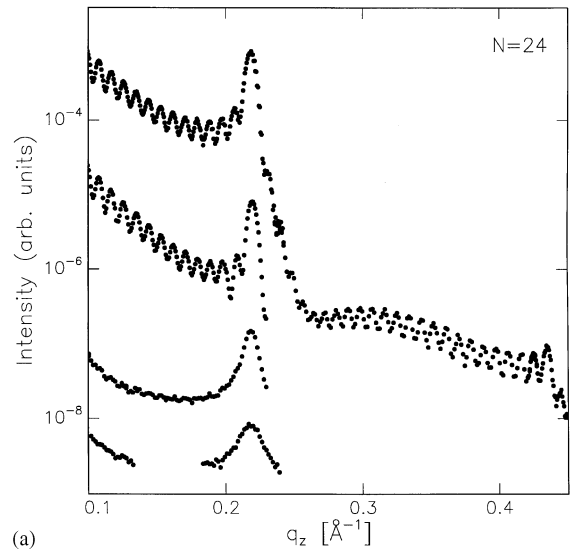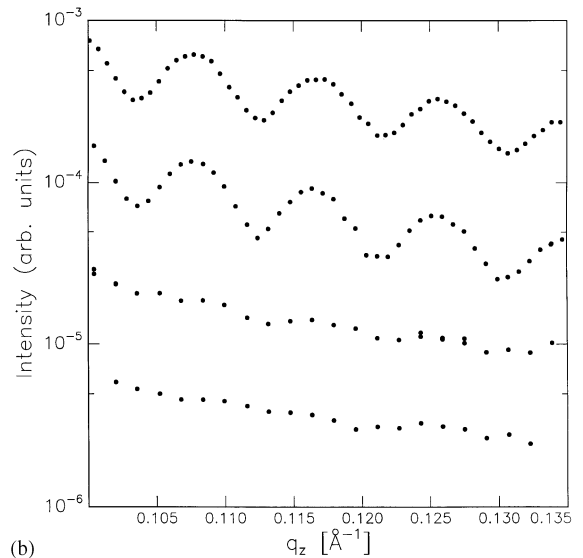

Fig. 5. Specular ($q_y = 0$, upper curves) and diffuse longitudinal scans for a 24 layer film with from top to bottom $q_y = 0$, $q_y = 0.0064 \, \text{Å}^{-1}$, $q_y = 0.0191 \, \text{Å}^{-1}$ and $q_y = 0.0414 \, \text{Å}^{-1}$ for a 24 layer film. Curves have been shifted for clarity; (a) q_z-range up to Bragg peak; (b) a magnification of small q_z range.

between more distant layers are constructively interfering, confirms that conformality between top and bottom of the film is lost. For short in-plane distances ($R \lesssim 40 \, \text{Å}$) the diffuse intensity seems to decay logarithmically with decreasing distance.
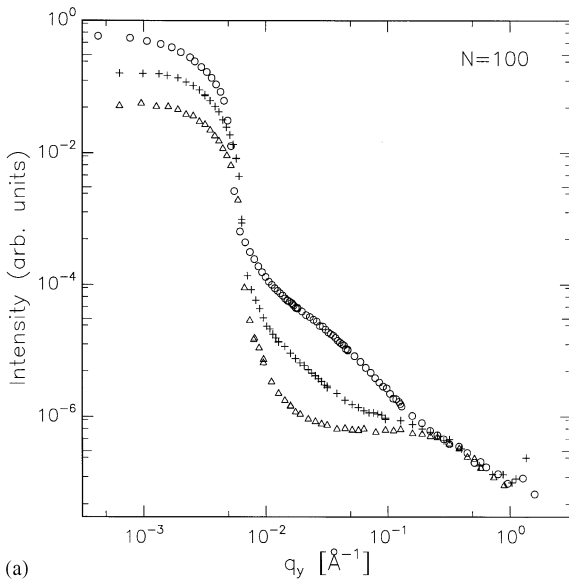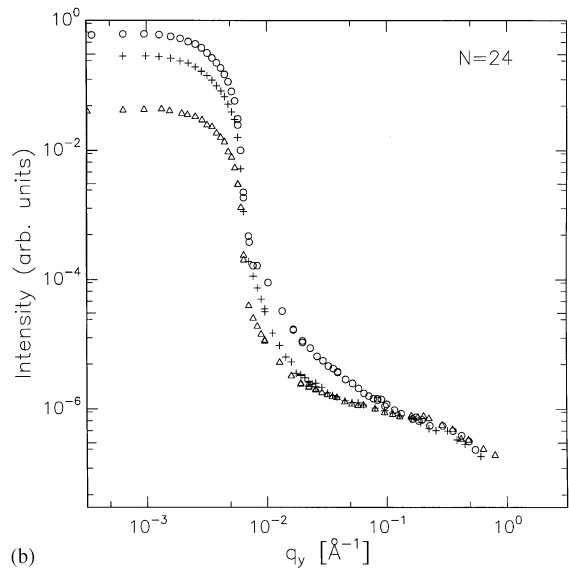
Fig. 6. Transverse diffuse scans for (a) a 100 layer film; (b) a 24 layer film, at the positions $q_z = 0.218\,\text{Å}^{-1}(q_0)$ (dots), $q_z = 0.109\,\text{Å}^{-1}(0.5q_0)$ (crosses) and $q_z = 0.152\,\text{Å}^{-1}(0.7q_0)$ (triangles).

In this regime of short lateral distances correlations between individual molecules are probed.

A critical comparison of the data to continuum theory [6,5] has been presented in Ref. [12]. Although, the fits show the same general trend as the data, at larger q_y considerable deviations exist, especially for the 100 layer film. In general, it was not possible to fit the whole set of scans in Fig. 5 with one value for σ_{loc}. A possible explanation might be in the results of Fig. 3, which indicates a strong profile of σ_{tot}. For the obtained values of B, K and γ [12] the amplitudes of the thermal fluctuations, σ, are 3.4 Å at the surface and 3.7 Å at the centre of the 24 layer film. Therefore, the thermal fluctuations hardly have a profile. Thus, using $\sigma_{\text{tot}}^2 = \sigma_{\text{loc}}^2 + \sigma^2$, the profile is mainly due to the local disorder with amplitudes of 5.3 and 0.9 Å at the interior and surface of the film, respectively. This strongly suggests the existence of a profile in the smectic order parameter. However, B is proportional to the square of the smectic order parameter [1]. Therefore, a profile of B in the film would not only influence the profile of the local fluctuational amplitude in the film, but also the correlations between the fluctuations. Such a profile of B has not yet been incorporated in the present continuum models, which could explain the discrepancies between theory and experiment.

5. Conclusions

X-ray specular reflectivity of freely suspended SmA films indicates a strong enhancement of the amplitude of the fluctuations in the interior of the films near thinning transitions, and proves the origin of melting to be in the interior of the film. Using diffuse X-ray scattering a crossover from conformal to independent fluctuations was observed in such films. The adapted scattering geometry for diffuse scattering at a synchrotron source, allowed us to determine the in-plane wave vector dependence of the hydrodynamic (collective) fluctuations down to in-plane length scales comparable to the lateral distances between molecules ($R \approx 4$–$5\,\text{Å}$). At decreasing length scales conformality between top and bottom of the film was progressively lost.

Acknowledgements

References

[1] See e.g. P.M. Chaikin, T.C. Lubensky, Principles of Condensed Matter Physics, Cambridge University Press, Cambridge, 1995; P.G. de Gennes, J. Prost, The Physics of Liquid Crystals, Clarendon Press, Oxford, 1993.

[2] J. Als-Nielsen et al., Phys. Rev. B 22 (1980) 312.

[3] E.I. Demikhov, V.K. Delganov, K.P. Meletov, Phys. Rev. E 52 (1995) 1285.

[4] T. Stoebe, P. Mach, C.C. Huang, Phys. Rev. Lett. 73 (1994) 1384.

[5] J.D. Shindler, E.A.L. Mol, A.N. Shalaginov, W.H. de Jeu, Phys. Rev. Lett. 74 (1995) 722; E.A.L. Mol, J.D. Shindler, A.N. Shalaginov, W.H. de Jeu, Phys. Rev. E 54 (1996) 536.

[6] R. Holyst, D.J. Tweet, L.B. Sorensen, Phys. Rev. Lett. 65 (1990) 2153; R. Holyst, Phys. Rev. A 44 (1991) 3692; A. Poniewierski, R. Holyst, Phys. Rev. B 47 (1993) 9840; V.P. Romanov, A.N. Shalaginov, Sov. Phys. JETP 75 (1992) 483; A.N. Shalaginov, V.P. Romanov, Phys. Rev. E 48 (1993) 1073.

[7] K.W. Evans-Lutterodt, M.T. Tang, J. Appl. Crystallogr. 28 (1995) 318.

[8] E.F. Gramsbergen, W.H. de Jeu, J. Chem. Soc. Faraday Trans. II 84 (1988) 1015.

[9] T. Salditt, T.H. Metzger, J. Peisl, Phys. Rev. Lett. 73 (1994) 2228; T. Salditt, T.H. Metzger, J. Peisl, G. Goerig, J. Phys. D 28 (1195) A236.

[10] C. Gourier et al., Phys. Rev. Lett. 78 (1997) 3157.

[11] M. Knewtson, R.M. Suter, J.D. Shindler, Reflectivity program SPEEDO.

[12] E.A.L. Mol et al., Phys. Rev. Lett. 79 (1997) 3439.

[13] S. Garg, K.A. Crandell, Phys. Rev. E 48 (1993) 1123.

[14] See e.g. L.V. Mirantsev, Phys. Lett. A 205 (1995) 412; T. Krancj, S. Žumer, J. Chem. Phys. 105 (1996) 5242; Y. Martinez, A.M. Somazo, L. Mederos, D. Sullivan, Phys. Rev. E 53 (1996) 2466.

[15] S.K. Sinha, Physica B 173 (1991) 25.